

Experimental Investigation of Impinging Axisymmetric Turbulent Fountains

Paul Cooper¹ and Gary R. Hunt²

¹School of Mechanical, Materials and Mechatronic Engineering, University of Wollongong, NSW 2522, Australia.
²Department Civil and Environmental Engineering, Imperial College London, London, SW7 2AZ, UK.

Abstract

The behaviour of a turbulent, axisymmetric, Boussinesq, vertical fountain that impinges on a horizontal plate a distance H from the fountain source is investigated. Images from Light Induced Fluorescence visualisation of the flow provide a clear picture of the internal structure of the impinging flow. The interaction between the impinging fountain and the plate results in a buoyant radial wall jet that spreads horizontally before separating from the surface at a radius R_{sp} . The transient development of the flow and behaviour of R_{sp} with time is described. The steady-state flow is modelled theoretically and a correlation of the non-dimensional spread of the impinging fountain is presented that successfully relates R_{sp}/H to the source-plate separation and the source characteristics of the fountain.

Background

The characteristics of turbulent plumes are of interest in many industrial and geophysical fluid flows. Frequently a prediction of the distribution of fluid density, velocity and concentration of contaminants, or other products, in the flow is needed for engineering design purposes. Plumes that develop from sources of buoyancy and momentum that act in opposite directions are known as fountains. Turner [1] reported experiments and presented an analytical model of a fountain developing in a uniform and quiescent environment. Baines, Turner and Campbell [2] extended this work to fountains within enclosures and determined the manner in which a fountain and a “filling box” interact. Bloomfield and Kerr [3] have more recently reported on the behaviour of axisymmetric and line fountains in an environment that is initially stratified.

The basic flow configuration for a positively-buoyant fountain developing in a homogeneous environment is shown in figure 1a. The outer, upward flowing, stream entrains fluid from both the surrounding ambient and from the downward moving buoyant jet. The focus of the present study is the situation where a fountain impinges on a horizontal plate as shown schematically in figure 1b. This situation is of interest both as a fundamental issue in fluid mechanics and also as the flow is central to a number of practical applications. The latter include the heating of large building spaces by warm jets of air directed downward from the ceiling (e.g. warm air curtains); flow from the jets of vertical takeoff aircraft; modelling of the dispersion of welding fume, as in gas metal arc welding (GMAW) where the plume of welding fume is initially directed downwards and outwards by shielding gas ejected from the GMAW nozzle towards the welding workpiece.

In the case of the impinging fountain, the buoyant fluid is forced radially outwards before rising as it impacts on the horizontal plate and thus the flow is wider than the free fountain (figure 1). The major objective the present work is to determine the way in which the presence of the solid plate changes the nature of the fountain and to investigate the flow both in the near field, close to the plate, and in the far field plume that rises above. Researchers who have looked at this problem and similar situations in the past include Lawrence and MacLachy [4] who investigated the radial spread of a positively-buoyant plume release beneath the surface

of a body of water. However, in this situation the stratification setup by the impinging plume is intrinsically stable, unlike the present case where the radial out-flowing jet (shown in figure 1b) is positively buoyant. More recently, Holstein and Lemckert [5] reported a set of experiments on impinging saline fountains. Their work focussed on how the radius of spread, R_{sp} , of the impinging fountain was related to the source conditions of the fountain, the source radius, R_0 , and source-plate separation, H .

Theoretical Framework

The two length scales that determine the behaviour of a free fountain, are the “jet length” ($l_M = M_0^{3/4}/B_0^{1/2}$) and the “acceleration length” ($l_Q = Q_0/M_0^{1/2} = \pi^{1/2}R_0$), where B_0 , Q_0 and M_0 are the source buoyancy, volume and specific momentum fluxes, respectively. The fountain source Froude number is then $Fr_0 = (l_M/l_Q)$. Turner [1] determined by experiment that the steady rise height, z_m , of a free fountain from a source with $Fr_0 \gg 1$ is given by $z_m = 1.85l_M$. In the present situation the distance of the source from the plate, H , represents the third length scale. The behaviour of the impinging fountain might therefore be expected to be determined by these three length scales and the source Reynolds number, $Re_0 = D_0V_0/\nu$, ($D_0 = 2R_0$).

After impinging on the plate one might expect the fountain to transform into a radial wall jet as discussed by many authors, e.g. Rajaratnam [6]. However, in the present case the radial outflow is positively buoyant and will separate from the plate when the Coanda effect has diminished sufficiently. In a 2D geometry, the separation distance between the source of a positively-buoyant wall jet flowing over a horizontal surface and the point where the jet detaches from the surface has been briefly reported by Sandberg *et al.* [7] who found the non-dimensional separation distance R_{sp}/H to be a function of the source Archimedes number, $Ar_0 = (Fr_0)^2$.

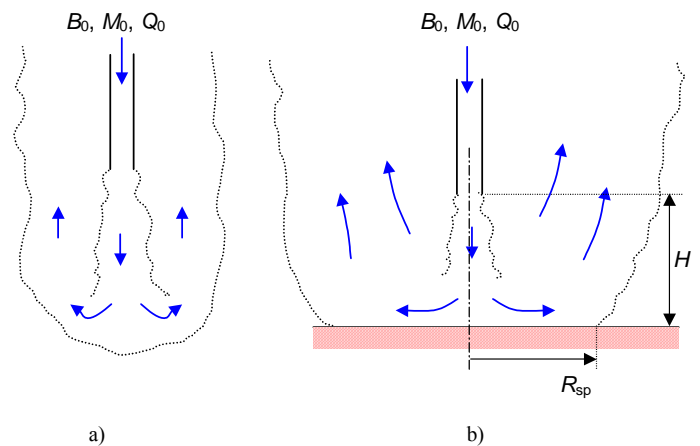


Figure 1. a) Turbulent fountain in a homogeneous environment; b) Turbulent fountain impinging on a horizontal plate.

In the present situation the impinging flow forms the “source” of the buoyant radial wall jet. Since we require $H \leq 1.85 l_M$ for a

fountain to impinge on the plate, we shall assume that at the plate the flow properties are similar to that of a free jet. In particular, the momentum flux at the plate (M_H) is approximately equal to that at the fountain source and the volume flux (Q_H) and velocity radius (b_v) are:

$$Q_H = 2^{3/2} \pi^{1/2} \alpha (H/l_Q) Q_0 \quad \text{and} \quad \frac{db_v}{dz} = 2\alpha \quad (1)$$

where $\alpha = 0.0535$ is the entrainment constant applicable to jets (Papanicolaou and List [8]) and z is the vertical coordinate with origin at the fountain source. We assume that a fraction, γ , of the vertical momentum of the mean flow in the down-flowing fountain is transformed to radial momentum in the radial wall jet. Invoking conservation of volume it can be shown that the source Archimedes number of the radial jet, $Ar_{rad} = g'_{rad} \delta_{rad} / u_{rad}^2$ is related to the Archimedes number of the source of the fountain, $Ar_0 = g'_0 R_0 / W_0^2$ as follows:

$$Ar_{rad} = 2^{5/2} \alpha^2 \gamma^{-3} (H/R_0)^2 Ar_0 \quad (2)$$

where g'_{rad} , δ_{rad} and u_{rad} are the buoyancy, thickness and velocity of the radial wall jet at its "source" at radius b_v , and g'_0 , R_0 and W_0 are the buoyancy, radius and velocity at the fountain source.

Experiments

Initial experiments were carried out at both the University of Wollongong and Imperial College London to determine the radius of spread (R_{sp}) of the radial wall jet. Preliminary experiments were visualised using a shadowgraph and then further experiments were conducted with sodium fluorescein dye added to the source fluid and the tank lit from below with a light sheet. The latter technique allowed the internal flow structure of the impinging fountains to be clearly visualised. A glass-walled tank measuring 1.4×1.4 m in plan was filled, with salt water as the ambient fluid, to a depth of approximately 1.2 m. A wide range of experiments were conducted with fresh water injected through nozzles with diameters between $3 \text{ mm} \leq D_0 \leq 10 \text{ mm}$, held at distances of $25 \text{ mm} \leq H \leq 200 \text{ mm}$ above the plate. The light sheet was generated by means of a line of dichroic incandescent 12v bulbs that were directed at a 1 mm wide slit in black cardboard sheeting attached to the lower glass surface of the tank. In the field of view it is estimated that the light sheet varied in thickness between 2 and 3 mm over the field of view. Images were captured by means of a digital CCD video camera (JAI CV-M4 monochrome, $1380(\text{h}) \times 1030(\text{v})$ pixel read out) and processed using the DigiFlow software system (Dalziel [9]).

Results and Discussion

The structure of the impinging fountain flow is somewhat different than might have been surmised from the observations of previous research that used shadowgraph or basic dyed fluid. The present Light Induced Fluorescence (LIF) experiments allowed a vertical section through the impinging fountain to be clearly visualised. Figure 2 is an enhanced and annotated image of a typical experiment taken after the flow had reached a quasi-steady state and shows the main flow features. One of the most striking features of the flow (as observed for $H/l_M \ll 1$) is that when the buoyant radial jet separates from the plate it does not form a line plume (circular in plan), but rather the separated flow is re-entrained into the radial outflow and the descending fountain forming a large toroidal vortex. After the initial transients, which are discussed in more detail below, a steady, turbulent plume rises above the toroidal vortex. The initial radius of this plume varies considerably with time during the transients.

The basic flow structure of the impinging fountain was found to depend primarily on the non-dimensional nozzle-plate separation,

H/l_M . Figure 3 shows examples of the different flow structures once steady state had been reached. The majority of the results presented herein are for experiments where $H/D_0 \gg 1$.

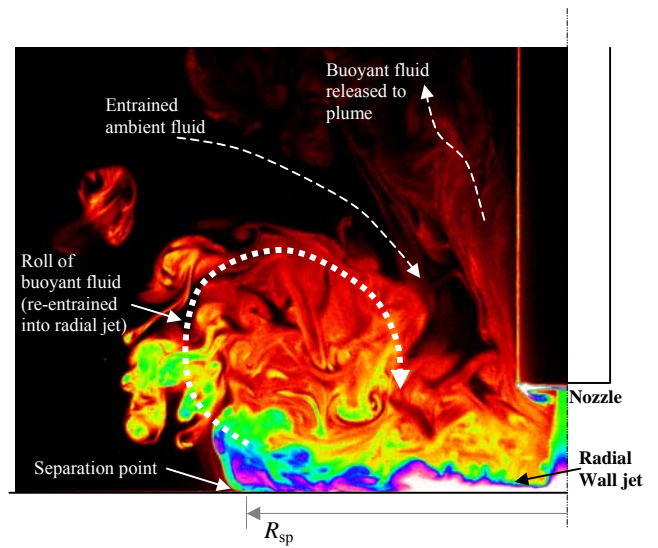


Figure 2. Digitally enhanced/annotated image illustrating the main characteristics of the flow field (only left half shown for clarity). $H/l_M = 0.10$, $H/D_0 = 8.3$.

For $H/l_M \ll 1$ the steady-state flow behaved in a fashion similar to that of an energetic, isothermal, turbulent jet impinging on a plate. Outside the impingement zone the thickness, δ , of the radial jet appeared to increase linearly with radius, r , as shown in figure 4. (However, one might expect the rate of growth, $d\delta/dr$, to be greater since the radial jet shear layer is effectively unstably stratified in the case of impinging fountains, as compared to the usual isothermal or filling box situations). Vortices aligned circumferentially were generated in the jet impingement zone and swept outward. These are visible in figure 4. The presence of these vortices cause the high local turbulence intensities reported by Cooper *et al.* [10] and other researchers investigating isothermal impinging jets. With increasing radius the buoyancy forces became dominant and resulted in the separation of the buoyant radial jet from the plate at the critical radius R_{sp} .

The transient development of the impinging fountains showed that for $H/l_M < 1.5$ there were three distinct stages of development as illustrated in the sequence of images in figure 5.

i) First, the starting fountain impacts with the plate and the horizontal radial flow is established. The front of the radial jet-like flow is a vortex ring, the major radius of which increases with time. The front observed is quite different from that observed for the spreading gravity current arising from an impinging, negatively buoyant plume (as in the case of the classic "filling box" situation, for example). During this initial transient very little buoyant fluid escapes re-entrainment and the majority is drawn back into the axisymmetric down-flowing fountain and radial outflow. Moreover, the ambient fluid immediately adjacent to the down-flowing fountain is co-flowing with the respect to the radial jet at this time.

ii) The separation radius of the attached radial jet reaches a maximum. At approximately this point in time a bulk upward motion of buoyant fluid occurs above the zone $r < R_{sp}$, and a starting plume develops with the radial jet acting as a distributed source of buoyancy.

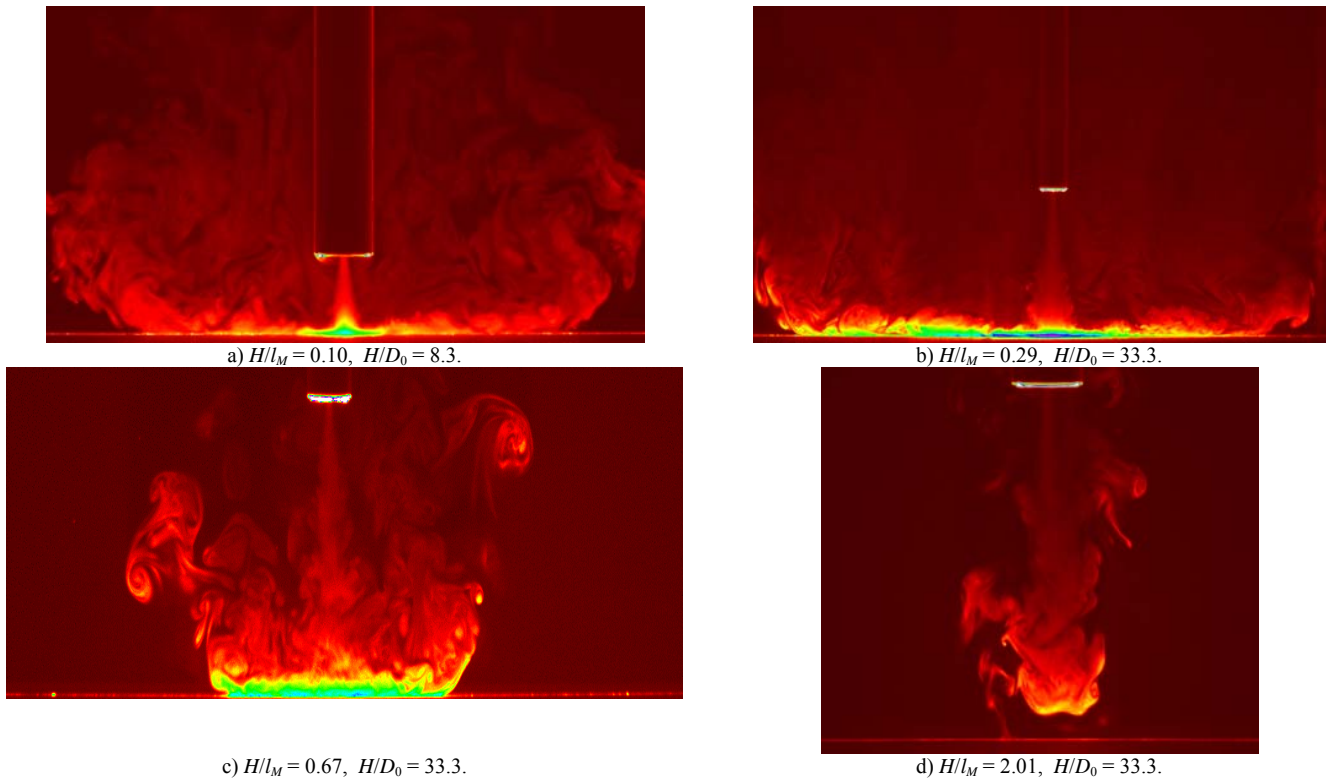


Figure 3. Structure of impinging fountain flow for a range of non-dimensional plate-nozzle separations under quasi-steady state conditions.

iii) Finally, the bulk plume flow above the nozzle, $z > H$, acts to reduce, and sometimes reverse, the direction of flow of ambient and re-entrained buoyant fluid adjacent to the fountain. Thus, the momentum flux of the fountain when it reaches the plate is reduced and the separation radius decreases and settles to a quasi-steady-state value.

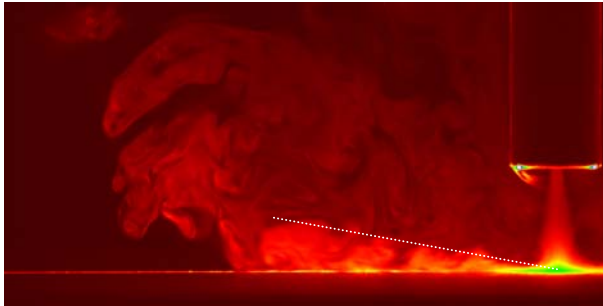


Figure 4. Buoyant radial wall jet development. $H/l_M = 0.10$, $H/D_0 = 8.3$.

A time-series image showing the variation of R_{sp} with time is shown in figure 6. This image was generated by processing the digital movie of a typical experiment so that a horizontal line of pixels just above the flat plate has been extracted from each frame of the movie and placed one above the other to give time on the vertical axis and a well-defined horizontal boundary indicating R_{sp} . For the case shown $R_{sp} \approx 240\text{mm}$ at 120s.

With increasing H/l_M the radial jet becomes thicker and less energetic, and the non-dimensional radius of separation, R_{sp} , decreases until at approximately $H/l_M \sim 2$ the fountain no longer maintains continuous contact with the plate, as shown in figure 3c. When the nozzle-plate separation $H/l_M \sim 2$ the fountain initially makes contact with the plate but subsequently detaches and may make periodic contact in the quasi-steady state.

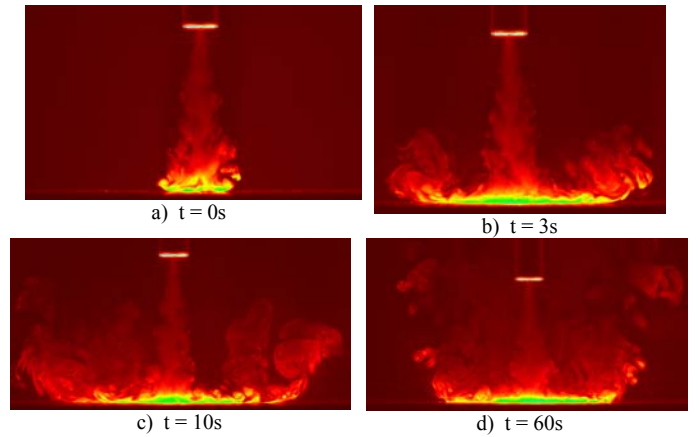


Figure 5. Initial development of the impinging fountain flow field for $H/l_M = 0.69$, $H/D_0 = 20.0$.

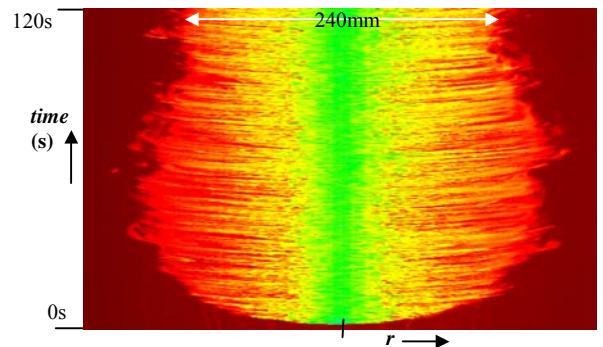


Figure 6. Typical time series of the intensity of light viewed in a line just above the flat plate for $H/l_M = 0.69$, $H/D_0 = 20.0$.

Figure 7 is a time-series image showing this transient. The figure was generated by taking a vertical line of pixels from the nozzle outlet to the plate from each frame of the digital movie of the experiment shown in figure 3d.

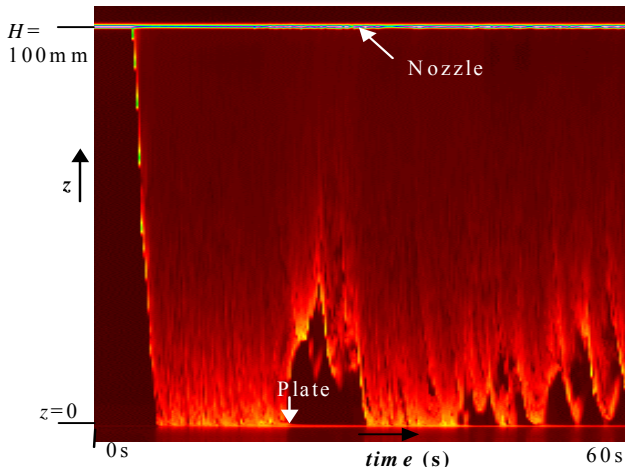


Figure 7. Time series of the intensity of light viewed in a vertical line between the nozzle outlet and the plate ($H/l_M = 2.01$ $H/D_0 = 33.3$).

The non-dimensional spread of the radial jet is successfully correlated by the scaling developed by the present authors as discussed above. Figure 8 shows a plot of the data from virtually all the shadowgraph experiments carried out over a wide range of source conditions and nozzle-plate separations. The solid line in this figure has a gradient of -0.75 which is the same as found by Sandberg *et al.* [7] for the case of a simple 2D buoyant jet introduced with horizontal momentum immediately above a horizontal surface. The numerical value of γ has a very strong influence on the properties of the radial jet (thickness, velocity, etc) and on the relationship between the Archimedes number of the fountain source and the radial jet source. A value of $\gamma \sim 0.3$ correlates the data most closely with that of Sandberg (which is for a different geometry). This is also consistent with the work of Witze and Dwyer [11] who found that assuming conservation of momentum “severely overpredicts” the radial jet momentum.

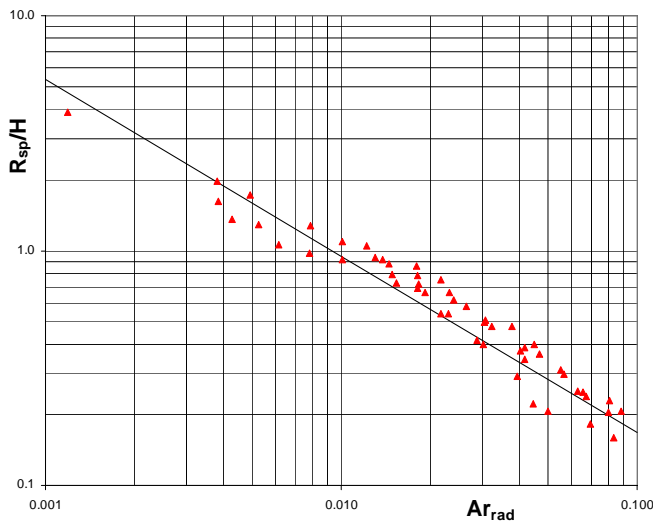


Figure 8. Radial spread of the buoyant radial jet as a function of the Archimedes number at the radial jet ‘source’ deduced from the source conditions of the fountain and assuming $\gamma = 1$ in (2). Symbols are experimental data and the solid line is a best fit with gradient -0.75 (the same power law dependency as reported in Sandberg *et al.* [7] for the separation of a plane buoyant jet injected across a horizontal surface).

The maximum Archimedes number in the experiments is $Ar_{rad} \sim 0.01$. This is the maximum value (approx.) for impinging fountains since it can be shown to be equivalent to a non-dimensional nozzle-plate separation of $H/l_M \sim 1.7$ beyond which the fountain will no longer impinge on the plate in a steady manner (*cf.* Turner [1]).

Conclusions

This work has shown that the flow structure within a fountain impinging on a horizontal plate is complex and is primarily dependent on the fountain source Archimedes (or Froude) number and the non-dimensional separation H/l_M of the nozzle and plate. The impinging fountain generates a buoyant radial wall jet that spreads out across the plate until buoyancy forces overcome the effects of momentum and the flow separates from the plate at a radius R_{sp} .

Light Induced Fluorescence experiments have shown that the upward flow from the impinging fountain cannot be modelled as a line plume arising from a ring of radius R_{sp} , owing to re-entrainment of the separating fluid by the fountain and radial jet.

The authors have developed a theoretical framework whereby the steady-state spreading radius (R_{sp}) of an impinging fountain may be predicted from the fountain source Archimedes number.

The transient development of the impinging fountain has been investigated and it is found that the fountain reaches the quasi-steady separation radius after an initial period where the plume rising from the impingement zone is not fully developed, thus, the separation radius is initially larger than in the steady state since the ambient fluid is co-flowing with, rather than counter-flowing against, the vertical fountain flow.

Acknowledgments

The authors would like to acknowledge the Engineering and Physical Sciences Research Council (UK) for partial support of the work described herein. They would also like to thank G.R.Slater and M.Gaston for carrying out the shadowgraph experiments. We are grateful to William Bobinski and Tony Allen at IC for constructing apparatus for the LIF experiments.

References

- [1] Turner, J. S., Jets and plumes with negative or reversing buoyancy, *J. Fluid Mech.*, **26**, 1966, 779-792.
- [2] Baines, W. D., Turner, J. S. and Campbell, I. H., Turbulent fountains in an open chamber, *J. Fluid Mech.*, **212**, 1990, 557-592.
- [3] Bloomfield, L. J. and Kerr, R. C., Turbulent fountains in a stratified fluid, *J. Fluid Mech.*, **358**, 1998, 335-356.
- [4] Lawrence, G. A. and MacLachy, M. R. Radially spreading buoyant flows, *J. Hydraulic Res.*, **39**, no. 6, 2001, 583-590.
- [5] Holstein, D. M. and Lemckert, C. J., Spreading of energetic submerged fountains impinging on a rigid surface, *Proc. 14th Australasian Fluid Mech. Conf.*, Adelaide, 2001, 749-752.
- [6] Rajaratnam, N. *Turbulent Jets*, Elsevier, 1976.
- [7] Sandberg, M, Wirén, B. and Claesson, L., Attachment of a cold plane jet to the ceiling – length of recirculation region and separation distance, *Proc. ROOMVENT 92*, Denmark, 1992, 489-499.
- [8] Papanicolaou, P. N. and List, E. J., Investigations of vertical turbulent buoyant jets, *J. Fluid Mech.*, **195**, 1988, 341-391.
- [9] Dalziel, S.B. Rayleigh-Taylor instability: experiments with image analysis. *Dyn. Atmos. Oceans*, **20**, 1993, 127-153.
- [10] Cooper, D., Jackson, D. C., Launder, B. E. and Liao, G. X., Impinging jet studies for turbulence model assessment – I. Flow-field experiments, *J. Heat Mass Transfer*, **36**, 1993, no. 10, 2675-2684.
- [11] Witze, P. O. and Dwyer, H. A., The turbulent radial jet, *J. Fluid Mech.*, **75**, part 3, 1976, 401-417.